

Lin Cao

Complex and Intelligent Systems Center,
East China University of Science and
Technology,
Shanghai 200038, China;
Department of Mechanical Engineering,
University of Saskatchewan,
Saskatoon, SK S7N 5A9, Canada
e-mail: lic909@mail.usask.ca

Allan T. Dolovich

Department of Mechanical Engineering,
University of Saskatchewan,
Saskatoon, SK S7N 5A9, Canada
e-mail: atd440@mail.usask.ca

Arend L. Schwab

Department of BioMechanical Engineering,
Delft University of Technology,
Delft NL 2628 CD, The Netherlands
e-mail: a.l.schwab@tudelft.nl

Just L. Herder

Department of Precision and
Microsystems Engineering,
Delft University of Technology,
Delft NL 2628 CD, The Netherlands
e-mail: j.l.herder@tudelft.nl

Wenjun (Chris) Zhang

Complex and Intelligent Systems Center,
East China University of Science
and Technology,
Shanghai 200038, China;
Department of Mechanical Engineering,
University of Saskatchewan,
Saskatoon, SK S7N 5A9, Canada
e-mail: wjz485@mail.usask.ca

Toward a Unified Design Approach for Both Compliant Mechanisms and Rigid-Body Mechanisms: Module Optimization

Rigid-body mechanisms (RBMs) and compliant mechanisms (CMs) are traditionally treated in significantly different ways. In this paper, we present a synthesis approach that is appropriate for both RBMs and CMs. In this approach, RBMs and CMs are generalized into modularized mechanisms that consist of five basic modules, including compliant links (CLs), rigid links (RLs), pin joints (PJs), compliant joints (CJs), and rigid joints (RJs). The link modules and joint modules are modeled through beam elements and hinge elements, respectively, in a geometrically nonlinear finite-element solver, and subsequently a beam-hinge ground structure model is proposed. Based on this new model, a link and joint determination approach—module optimization—is developed for the type and dimensional synthesis of both RBMs and CMs. In the module optimization approach, the states (both presence or absence and sizes) of joints and links are all design variables, and one may obtain an RBM, a partially CM, or a fully CM for a given mechanical task. Three design examples of path generators are used to demonstrate the effectiveness of the proposed approach to the type and dimensional synthesis of RBMs and CMs.
[DOI: 10.1115/1.4031294]

1 Introduction

Two major categories of mechanisms are RBMs and CMs. An RBM gains all of its motion from the relative movements between its rigid members through kinematic pairs or joints. In contrast, a CM gains at least part of its motion from the deformation of its deformable members [1]. This difference makes RBMs and CMs significantly different in analysis and synthesis. However, RBMs can be practically viewed as a CM because there is no absolutely rigid component. Along this line of thinking, a new approach to mechanism synthesis called module optimization is presented in this paper. Our general idea is not to distinguish between RBMs and CMs, and a component in a mechanism (regardless of RBMs and CMs) is thus called a module. Further, with this approach, there is no separation of type synthesis and dimensional synthesis, while the two design activities are indeed separated in traditional mechanism design theory.

In traditional mechanism design theory, type synthesis involves determining a proper mechanism topology to best suit a desired

mechanical task [2]. The “topology” here includes the number of links and joints, the types of the joints, the connectivity of the links and the joints, the types and locations of inputs, and the displacement boundaries (ground) [3,4]. Dimensional synthesis involves determining the geometry of a mechanism to accomplish a specified task [1]. Approaches to type synthesis and approaches to concurrent type and dimensional synthesis can be found in the literature for both RBMs and CMs [5–20].

A typical approach to the type synthesis of RBMs is to enumerate the basic kinematic chains based on a matrix representation of mechanism topology and to perform analysis based on graph theory [3,21,22]. The number and the connectivity of links and joints are to be determined. This approach has also been extended for the type synthesis of CMs [23]. It is clear that type synthesis only accomplishes a partial design task.

Two approaches are available for the concurrent type and dimensional synthesis of RBMs. One is based on a truss ground structure model [6,7,9], and the other is based on a spring-connected rigid block model [10]. In the first approach, a network of rigid truss links is used to initialize a design domain. By iteratively removing links in the design domain, the remaining truss links form an RBM with determined topology and dimensions. This approach can be called a link determination approach as the final topology of an RBM is determined by the remaining links in

Contributed by the Mechanisms and Robotics Committee of ASME for publication in the JOURNAL OF MECHANICAL DESIGN. Manuscript received January 6, 2015; final manuscript received July 19, 2015; published online October 15, 2015. Assoc. Editor: Charles Kim.

the design domain. In the second approach, rigid blocks, in a design domain, are connected through zero-length springs. By keeping or removing some of these springs, the connectivity among the rigid blocks can be determined: disconnected, rigidly connected, or connected through PJs. Note that blocks or links are not removed in this approach, and the topology of a mechanism is only determined by the remaining springs (joints). The approach can thus be called a joint determination approach.

Ananthasuresh [11] pioneered the type and dimensional synthesis of CMs based on topology optimization that was originally used for stiff structures. Topology optimization was then further developed based on a truss (truss-only) ground structure model [14] and a beam (beam-only) ground structure model [12,13]. Ramrakhyani et al. [15] developed a type of hinged-beam element that has a PJ at one end and an RJ on the other end. Similar to the truss ground structure approach for RBM synthesis, approaches for the synthesis of CMs based on the truss-only, beam-only, and hinged-beam ground structure models can be viewed as a link determination approach because the final design is determined by the remaining links in the design domain.

The purpose of this study was to extend the topology optimization technique to an integrated link and joint determination approach called module optimization for the type and dimensional synthesis of both RBMs and CMs. RBMs and CMs were modularized into a general mechanism that comprises link modules and joint modules, including CLs, RLs, PJs, CJs, and RJs. The assembly of these modules forms the topology and dimension of a mechanism. A new beam-hinge model based on the planar beam element and hinge element in SPACAR (a finite-element program originally developed at the TU Delft, Delft, The Netherlands [24]) was proposed to represent the link modules (beam elements) and joints modules (hinge elements). A design domain is initialized with both beam elements (for links) and hinge elements (for joints). By determining the state (absence, CL, or RL) of each link and that (PJ, CJ, or RJ) of each joint, a mechanism can be obtained. The proposed approach for the synthesis of mechanisms has the following special features:

- (1) The approach is used for the concurrent type and dimensional synthesis of RBMs, partially CMs, and fully CMs. One may obtain an RBM, a partially CM, or a fully CM with this approach without any prescription of the type of mechanisms.
- (2) Designers are also able to select their desired category of mechanisms prior to the design process by prescribing the appropriate basic modules to be included in the design process. For example, if an RBM is desired, one may exclude the CL and CJ modules and prescribe RL, RJ, and PJ as basic modules to initialize design domains.
- (3) The approach provides a new perspective on the relationship between RBMs and CMs: their designs can be unified, which is philosophically correct because the rigid body is just an assumption on the bodies with ignorable deformations.
- (4) The approach is a combined link and joint determination approach. The states of links and those of joints are all design variables, while the joint determination approach and link determination approach predetermine the states of links and states of joints, respectively.
- (5) Rotational input motion can be specified in a natural way due to the advantage of the proposed beam-hinge model (refer to Sec. 4.1 for details). This feature facilitates the synthesis of mechanisms (especially CMs) for more complicated motion tasks that are defined by rotational motion. In the literature, topology optimization techniques are used to design CMs for simple tasks such as amplifying motion or gripping [25], and the type of motion considered in topology optimization is mainly translational motion.
- (6) CJs are incorporated into the type and dimensional synthesis of CMs. CJs, such as flexure hinges and large-

displacement joints [26–30], are long considered in the architecture of CMs but have never been considered in the type and dimensional synthesis of CMs.

2 Modularization of RBMs and CMs

Figure 1(a) shows a four-bar RBM whose links are rigid and connected by PJs. By replacing the PJs with CJs, e.g., notch-type CJs, one can obtain a lumped four-bar CM, as shown in Fig. 1(b). The links in the lumped CM are relatively rigid but are connected by the notch-type CJs that permit relative rotation (through deformation) between the connected links. Instead of using CJs, a distributed four-bar CM, as shown in Fig. 1(c), consists of CLs that connect through RJs. RJs do not permit relative rotation or translation between the connected links, but the links are flexible and can be deformed throughout the bodies. Figure 1(d) is a partially compliant four-bar mechanism where the motion is due to the deformation of the compliant components and the relative rotation of the links permitted by the PJs. With these observations, these four-bar mechanisms can be generally viewed as an assembly of link modules and joint modules, as shown in Fig. 1(e). Link modules consist of RL modules and CL modules, and joint modules consist of PJ modules, CJ modules, and RJ modules. In general, as shown in Fig. 1(f), any type of mechanisms can be modularized as an assembly of link modules and joint modules. The type of a mechanism is determined by the types of modules and how the modules are connected.

3 Finite-Element Analysis Using SPACAR

A geometrically nonlinear finite-element solver SPACAR [24,31] was employed for mechanism analysis in this study. The special feature of this solver is that both links and joints can be modeled using specific finite elements, namely, beam elements and hinge elements, respectively. This section briefly introduces the fundamental concepts, beam element, and hinge element in SPACAR (refer to Refs. [24,31–33] for details).

3.1 Fundamental Concepts. A mechanism is divided into an assembly of finite elements. The configuration of an element is described by a set of nodal coordinates and deformation parameters. Nodal coordinates include the Cartesian coordinates and orientation coordinates. The Cartesian coordinates describe the position of an element in a global coordinate system, and the orientation coordinates describe the orientation of an element to its reference position (usually the initial position). A deformation parameter, defined as a function of the nodal coordinates of the element, describes the elastic deformations of the element or the relative rotations between two hinged elements. All the deformation parameters of the elements of a mechanism are described as

$$\boldsymbol{\varepsilon} = \boldsymbol{\varepsilon}(\mathbf{x}) \quad (1)$$

where \mathbf{x} is the vector of the nodal coordinates of all the elements that represent the mechanism, and $\boldsymbol{\varepsilon}$ is the vector of the deformation parameters. Both the nodal coordinates and deformation parameters can be classified into three categories: fixed ($\mathbf{x}^{(0)}, \boldsymbol{\varepsilon}^{(0)}$), specified as inputs ($\mathbf{x}^{(m)}, \boldsymbol{\varepsilon}^{(m)}$), and calculable unknowns ($\mathbf{x}^{(c)}, \boldsymbol{\varepsilon}^{(c)}$) [24]. Equation (1) defines the equations for kinematic analysis where the vectors $\mathbf{x}^{(c)}$ and $\boldsymbol{\varepsilon}^{(c)}$ are to be calculated. Static analysis and dynamic analysis are performed based on the principle of virtual power, given the inertia/stiffness/damping properties (refer to Refs. [24,31] for details).

3.2 Planar Beam Element. The planar beam element in SPACAR, as shown in Fig. 2(a), has two end nodes, p and q . Each node has two Cartesian coordinates and one orientation coordinate; the vector of the nodal coordinates is

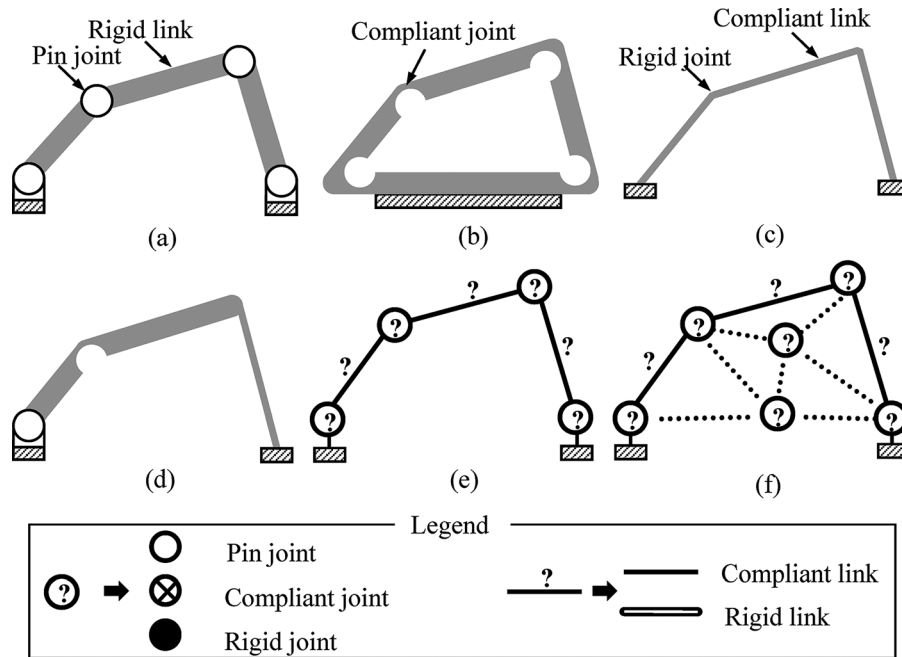


Fig. 1 Modularization of mechanisms: (a) a four-bar RBM, (b) a four-bar lumped fully CM, (c) a four-bar distributed fully CM, (d) a four-bar partially CM, (e) a modularized four-bar mechanism with link and joint modules, and (f) a general modularized mechanism with link and joint modules (the dotted lines represent any possible connectivity). Note that the symbols for the five modules are used hereafter in this paper.

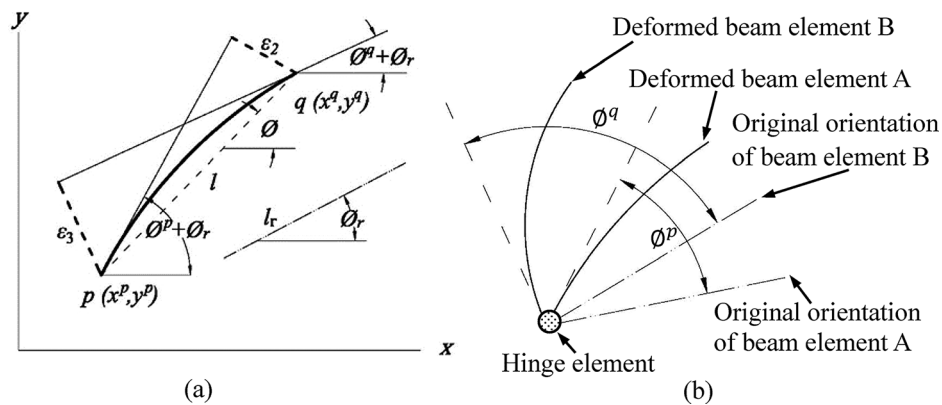


Fig. 2 Definitions of beam and hinge elements: (a) the coordinates and deformation parameters of the beam element and (b) the hinge element between two connected beam elements

$$\mathbf{x} = \begin{bmatrix} \mathbf{x}^p \\ \mathbf{x}^q \end{bmatrix} = [\mathbf{x}^p, \mathbf{y}^p, \varnothing^p | \mathbf{x}^q, \mathbf{y}^q, \varnothing^q]^T \quad (2)$$

where (x^p, y^p) and (x^q, y^q) are the Cartesian coordinates describing the positions of the element, and \varnothing^p and \varnothing^q are the orientation coordinates which are defined based on a corotated coordinate system. Specifically, the orientation coordinates are defined respect to the reference orientation of the element, and they are attributed to both the rigid-body rotation and elastic deformation of the element. The rigid-body rotation, indicated by the corotated line (the dashed line) between nodes p and q , equals $\varnothing - \varnothing_r$, where \varnothing and \varnothing_r represent the instantaneous and original orientations of the corotated line, respectively. Thus, $\varnothing^p - (\varnothing - \varnothing_r)$ and $\varnothing^q - (\varnothing - \varnothing_r)$ represent the nodal orientation change at node p and q , respectively, due to the bending deformations ε_2 and ε_3 of the material. Another deformation parameter is ε_1 which describes the length change (elongation) of the element. The three deformation modes are calculated by

$$\begin{aligned} \varepsilon_1 &= ((x^q - x^p)^2 + (y^q - y^p)^2)^{1/2} - l_r \\ \varepsilon_2 &= \sin[(\varnothing^p - (\varnothing - \varnothing_r)) \cdot l] \\ \varepsilon_3 &= -\sin[\varnothing^q - (\varnothing - \varnothing_r)] \cdot l \end{aligned} \quad (3)$$

where l and l_r are the instantaneous length and original length of the element, respectively. Note that the deformation parameters in Eq. (3) are invariant with respect to rigid-body movements (rotation and translation) of the element [31].

3.3 Planar Hinge Element. The planar hinge element, with its axis perpendicular to the plane of described motion, describes the relative rotation between two hinged or connected beam elements, as shown in Fig. 2(b). The element has two orientation nodes (p and q), and each node has one orientation coordinate. The vector of the nodal coordinates of the element is

$$\mathbf{x} = [\varnothing^p, \varnothing^q]^T \quad (4)$$

where ϑ^p (ϑ^q) is the orientation coordinate of the node p (q). The orientation coordinates are defined with respect to the original orientations of the beam elements that are connected by the hinge element. The element has only one deformation mode

$$\varepsilon_1 = \vartheta^q - \vartheta^p \quad (5)$$

where ε_1 represents the relative rotation of the two connected beam elements. Note that both the planar beam element and planar hinge element can be defined with relevant stiffness properties.

4 Module Optimization of Mechanisms

This section introduces the module optimization of mechanisms. Section 4.1 proposes a new beam-hinge ground structure model and compares it with the conventional beam-only model. Section 4.2 introduces the design variables, followed by the principles for joint interpretation in Sec. 4.3. The objective function and constraints are introduced in Secs. 4.4 and 4.5, respectively.

4.1 Beam-Hinge Ground Structure Model. In this study, a new beam-hinge ground structure model for topology optimization was proposed based on the beam element and hinge element introduced in Sec. 3. The new beam-hinge model has two essential features compared with the widely used beam-only model in the ground structure approach for topology optimization. First, the joint stiffness between two connected beam elements can be described and thus controlled through the hinge element while the joint in the conventional beam-only model is simply assumed rigid. Second, the relative angle between the two connected beam elements can be explicitly described and actively varied through either the orientation coordinates or the deformation mode of the hinge element.

The two features can be demonstrated by an example. In the conventional beam-only model shown in Fig. 3(a), two beam elements A and B share the same rotation coordinate at node 3, i.e., θ^3 , which means that the relative angle between A and B is fixed. In other words, A and B are rigidly connected. In the beam-hinge model as shown in Fig. 3(b), A and B are connected at the translation node 3, and their orientation nodes 4 and 5 are connected through a hinge element C (a circle filled with black dots). The coordinates of 4 and 5 are ϑ^4 and ϑ^5 , respectively. The relative rotation between A and B is thus $\vartheta^5 - \vartheta^4$, which equals ε_1 of the hinge element. One can specify the relative rotation by specifying either ϑ^4 and ϑ^5 , or ε_1 . Given the relative rotation, the moment transferred between A and B is determined by the rotational stiffness of the hinge element C. In other words, the hinge stiffness determines how strongly A and B are connected (in the torsional direction).

The proposed beam-hinge model can be used to model the modularized mechanism. Link modules and joint modules can be represented with beam elements and hinge elements of different stiffness properties, respectively. Figure 4 shows the FEM representation of the modularized four-bar mechanism in Fig. 1(e).

Similarly, a design domain can be discretized or meshed using beam elements and hinge elements, as shown in Fig. 5. A group of points are selected to be connection points, and the beam elements are connected through the hinge elements at these points. The

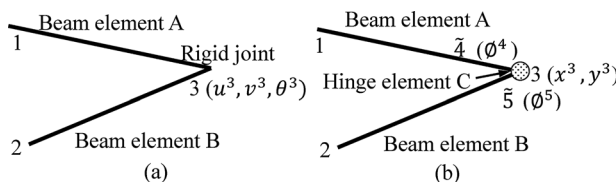


Fig. 3 Model comparison: (a) conventional beam-only model and (b) the proposed beam-hinge model

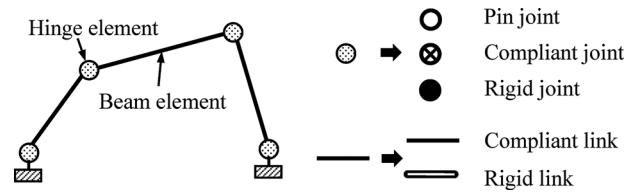


Fig. 4 Beam-hinge model of the modularized four-bar mechanism

stiffness of the beam elements and stiffness of hinge elements indicate the states of the links and states of the joints, respectively. Each link has three possible discrete states: removed from the domain, CL, or RL. Any removed link is assigned with a very small stiffness value. A CL also has three possible in-plane widths, and an RL is assigned with a relatively large bending stiffness and elongation stiffness (compared with CLs). Similarly, each joint also has three possible states: PJ, CJ, or RJ. A hinge element with zero torsional stiffness represents a PJ; a hinge element with a certain positive torsional stiffness represents a CJ; and a hinge element with infinite or fairly large stiffness represents an RJ. Note that an RL is only viewed as a piece of material with a relatively large stiffness. The type of the material and size (except the length) of an RL are not the concern in the present study and should be considered in the embodiment design.

Note that $n - 1$ hinge elements are required to describe the joints between n beam elements that are connected at the same location. One of these beam elements is selected as the reference beam element which connects to each of the other beam elements through a hinge element. To aid understanding, a dashed circle is used to indicate a multi-hinge region where multiple hinge elements exist at the same connection point (the center of the multi-hinge region). In a multi-hinge region, except for the reference element, each beam element is adjacent to a hinge element that connects the beam element to the reference element.

4.2 Design Variables. There are three groups of design variables. The first group of design variables is the continuous position variables, (x_p, y_p) , at the connection points. Each connection point could be at any position in a surrounding rectangular region, namely, the floating region. A floating region of the connection

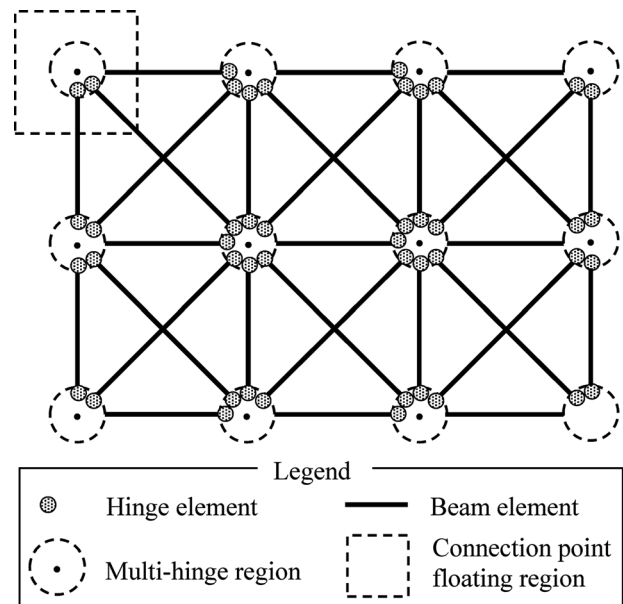


Fig. 5 Discretized design domain with the beam-hinge ground structure model

point is shown in Fig. 5 as a sample. A floating region provides a connection point with greater geometric freedom [34]. Note that these rectangular regions should not have any intersection with one another. The second group of design variables is the discrete state variables, \mathbf{L} , which represent the states of the links. The third group of design variables is the discrete state variables, \mathbf{J} , which represent the states of the joints. The ranges of these design variables are problem-specific (refer to Sec. 5 for some examples).

4.3 Joint Interpretation. The interpretation of joints is straightforward if the link represented by the reference beam element remains in the design domain, that is, each hinge element, in a one-to-one manner, represents one joint. However, this one-to-one manner of interpretation is not applicable when the reference link is absent or removed from the design domain. As shown in Fig. 6(a), three beam elements A, B, and C are connected at connection point 1. Element A is the reference beam element which is directly connected to B and C through hinge elements d and e , respectively. Note that in this way, B and C are indirectly connected. As shown in Fig. 6(b), one design may end up with link A being removed while B and C being kept in the design domain, and the joints represented by hinge elements d and e are a CJ and an RJ, respectively. The two joints are connected in series and indirectly represent the connection between B and C. In practice, however, the joint connection between B and C must be directly described by one joint module. Thus, the combination of a CJ and an RJ is now interpreted as a CJ, as shown in Fig. 6(c). This is so because a CJ is functionally equivalent to an RJ and a CJ that are connected in series. The principles for the interpretation of any two joint modules are schematically shown in Fig. 7.

4.4 Objective Function. The design problem in this study is to find the type and dimension of a mechanism, either an RBM or a CM, so that the mechanism follows a prescribed or desired path when actuated by a rotational input motion. Thus, the functional requirement in this case is path generation, i.e., the control of a point on a mechanism such that it follows a prescribed path [35]. Thus, the objective function is to minimize the mean distance between the desired path and the generated path

$$\text{Minimize mean distance} = \frac{1}{n} \sum_{i=1}^n d_i \quad (6)$$

where n is the number of selected precision points on the desired path, and d_i is the distance from a precision point i to the generated path of a mechanism candidate. The mean distance is schematically shown in Fig. 8. The general idea is to determine the mean distance from the selected precision points on the desired path to the generated path.

4.5 Constraints. The purpose of the module optimization in the present study was

to find: $\mathbf{x}_p, \mathbf{y}_p, \mathbf{L}, \mathbf{J}$

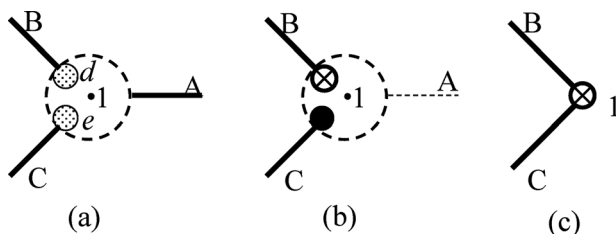


Fig. 6 Joint interpretation when the reference link is absent: (a) the mesh with beam elements and hinge elements, (b) the design with the referenced link A being removed, and (c) the interpretation of the design in (b)

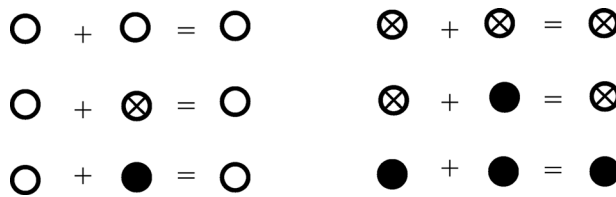


Fig. 7 Principles for the interpretation of two joints that are connected in series. In each principle, the first term represents the joint between link B and the reference link A, and the second term represents the joint between link C and the reference link A. The third term represents the joint between B and C when A is absent.

$$\text{to minimize } \frac{1}{n} \sum_{i=1}^n d_i$$

subject to

Valid connectivity check

$$\begin{aligned} \mathbf{x}_p^{\text{lower}} &\leq \mathbf{x}_p \leq \mathbf{x}_p^{\text{upper}} \\ \mathbf{y}_p^{\text{lower}} &\leq \mathbf{y}_p \leq \mathbf{y}_p^{\text{upper}} \\ 1.5 &< \lambda_{\text{buckling}} \\ |\sigma_{\text{maxCL}}| &< [\sigma] \\ |\epsilon_{\text{maxCJ}}| &< [\epsilon_{\text{CJ}}] \\ |\epsilon_{\text{maxRJ}}| &< [\epsilon_{\text{RJ}}] \\ |\theta_{\text{maxRL}}| &< [\theta_{\text{RL}}] \end{aligned} \quad (7)$$

Some notes on Eq. (7) are given below:

- (1) Valid connectivity check was performed for each candidate design to ensure the connections between the input port, the output port, and the displacement boundaries of a mechanism.
- (2) \mathbf{x}_p and \mathbf{y}_p are the vector of the horizontal coordinates and that of the vertical coordinates of the connection points, respectively. \mathbf{x}_p range from $\mathbf{x}_p^{\text{lower}}$ to $\mathbf{x}_p^{\text{upper}}$, and \mathbf{y}_p range from $\mathbf{y}_p^{\text{lower}}$ to $\mathbf{y}_p^{\text{upper}}$.
- (3) \mathbf{L} and \mathbf{J} are the vectors of the design variables of the links and the joints, respectively.
- (4) $\lambda_{\text{buckling}}$ is the critical buckling load multiplier which equals the critical buckling load over the input force or torque. $\lambda_{\text{buckling}}$ is constrained to be larger than 1.5. This constraint is imposed to ensure that the applied input force or torque was not large enough to buckle the mechanism (refer to Ref. [36] for details).
- (5) $|\sigma_{\text{maxCL}}|$ and $[\sigma]$ are the maximum stress (absolute value) of a mechanism on all CLs and the yield strength of the material used, respectively. The stress is the normal stress due to bending and axial loadings.

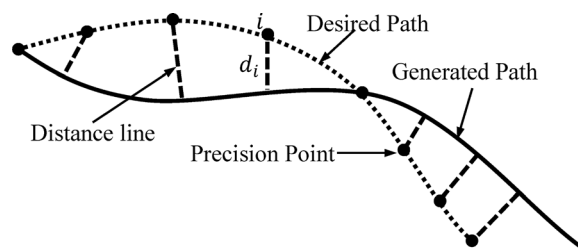


Fig. 8 Desired path and generated path

- (6) $[\varepsilon_{\max_{CJ}}]$ and $[\varepsilon_{CJ}]$ are the maximum deformation (absolute value) of CJs and the deformation limit, respectively. A CJ can only rotate in a limited range, depending on the structure of the CJ. For instance, the Free-Flex[®] Pivot (a CJ) designed by Riverhawk Company can travel up to 60 deg [37].
- (7) $|\theta_{\max_{RL}}|$ and $[\theta_{RL}]$ are the maximum angular rotation (absolute) and the rotation limit of RLs. An RL has two bending modes: ε_2 and ε_3 . The angular rotations due to bending deformation are $\theta_2 = \varepsilon_2/l$ and $\theta_3 = \varepsilon_3/l$, where l is the instantaneous length of the RL. In this study, each RL is implicitly modeled using a beam element with high stiffness and with deformation modes being released (i.e., free to be deformed). The beam element is supposed to function as an RL by implicitly suppressing deformation. However, RLs may be undesirably deformed due to inappropriate topologies or dimensions. This constraint limits the undesirable deformation of RLs to negligible small deformation.
- (8) $[\varepsilon_{\max_{RJ}}]$ and $[\varepsilon_{RJ}]$ are the maximum deformation (absolute value) and the deformation limit of RJs, respectively. This constraint limits the undesirable deformation of RJs to negligible small deformation.

Note that the constraints on RLs and RJs and the strength constraint on CLs ensure that the mobility of a mechanism mainly comes from the bending of CLs, the relative rotation permitted by PJs, and the deformation of CJs.

The optimization problem was solved using the genetic algorithm in the Global Optimization Toolbox in MATLAB [38]. The toolbox can solve optimization problems that have both continuous and discrete variables [39].

5 Design Examples

Three design examples are presented to demonstrate the effectiveness of the proposed module optimization technique. The three examples aim to design an RBM, a fully CM, and a partially CM, for the same path generation task with the selected modules.

Design specifications on design parameters, design variables, beam elements, and hinge elements are introduced in Sec. 5.1, followed by a description of the three design examples in Sec. 5.2.

5.1 Design Specifications. The space has an area of $400 \times 400 \text{ mm}^2$, with a grid of 3×3 nodes, creating 20 beam elements and 31 hinge elements, as shown in Fig. 9. Each block has an area of $200 \times 200 \text{ mm}^2$, and the location of each connection point is allowed to vary in a floating region of $190 \times 190 \text{ mm}^2$ surrounding it. Tables 1 and 2 list the design parameters and design variables, respectively. The state of each link module is represented by the in-plane width of its beam element, as presented in Table 3. The in-plane width and the Young's modulus of each absent link were $1 \times 10^9 \text{ mm}$ and $1 \times 10^{-13} \text{ Pa}$, respectively, for two reasons: (1) the stiffness of an absent link must be small enough to be negligible and (2) no buckling failure on an absent link if its $EA \ll EI$, where E , A , and I are the Young's modulus, the cross-sectional area, and the moment of inertia, respectively. EA and EI represent the axial rigidity and the flexural rigidity (in the bending direction), respectively. The values of the torsional stiffness of the hinge elements for PJs, CJs, and RJs were 0, 0.006, and 2.460 (unit: $\text{N} \cdot \text{m}/\text{rad}$), respectively. The stiffness of CJs was selected so that the flexural rigidity of CJs and that of CLs were on the same level. The stiffness of RJs and the in-plane width of RLs were selected so that their flexural rigidity was far larger than those of CJs and CLs.

5.2 Design Illustrations. The three examples are to design an RBM, a fully CM, and a partially CM, respectively, for the same path generation problem with selected modules. In the first example, RL, PJ, and RJ modules are selected to be the basic modules in design; in the second example, except the PJ module, all other

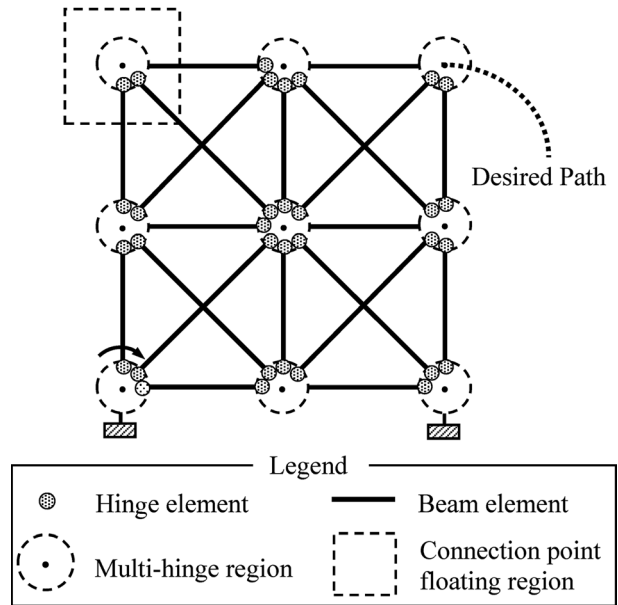


Fig. 9 Design domain

Table 1 Design parameters

Material	Polypropylene
Young's modulus	1.4 GPa
Yield strength	32.2 MPa
Out-of-plane depth	10 mm
Input rotation	$-\pi/3$ rad (clockwise)
$[\varepsilon_{CJ}]$	$\pi/3$ rad
$[\varepsilon_{RJ}]$	$\pi/180$ rad
$[\theta_{RL}]$	$\pi/180$ rad

modules are selected as basic modules, in the third example, all the five modules are selected as basic modules. The desired path is defined as the curve of a quadratic function

$$y = -10(x - x_{\text{output}})^2 + y_{\text{output}}, \quad x \in [x_{\text{output}}, x_{\text{output}} + 0.12] \quad (8)$$

where (x, y) is the position coordinates of points on the curve, and $(x_{\text{output}}, y_{\text{output}})$ is the initial position coordinates of the output port of a mechanism. The curve was defined to make the shape and size of the curve independent from the initial position (considered as design variables in the study) of the output port of a mechanism. Note that the change in the x -coordinate from the start to the end of the output path is 120 mm which is 30% of the characteristic length (400 mm) of the design domain.

6 Results and Discussion

Design results using the genetic algorithm for examples I–III are listed in Fig. 10. The first column shows both the absent links and the present links in the results, generated paths, and desired paths. The in-plane widths of links are denoted by the widths of lines. The second column shows both the link and joint modules in the design results. The first row to the third row represents the design results for examples I, II, and III, respectively. The values of the objective functions of the three results are 0.0054, 0.0020, and 0.0017, respectively.

The interpretation of the result of example I is depicted in Fig. 11. The link and joint modules of the original resulting mechanism (Fig. 11(a)) are interpreted into the configuration shown in Fig. 11(b) according to the joint interpretation principles. The

Table 2 Design variables. (x_{pi}^0, y_{pi}^0) is the floating region center of connection point i ; CL-1, CL-2, and CL-3 indicate the three different in-plane widths of the CLs.

Number	Variable	Type	Possible values or range
1	x_{p1}	Continuous	$[x_{p1}^0 - 95, x_{p1}^0 + 95]$ mm
...
9	x_{p9}	Continuous	$[x_{p9}^0 - 95, x_{p9}^0 + 95]$ mm
10	y_{p1}	Continuous	$[y_{p1}^0 - 95, y_{p1}^0 + 95]$ mm
...
18	y_{p9}	Continuous	$[y_{p9}^0 - 95, y_{p9}^0 + 95]$ mm
19	L_1	Discrete	0 (absent), 1 (CL-1), 2 (CL-2), 3 (CL-3), 4 (RL)
...
38	L_{20}	Discrete	0 (absent), 1 (CL-1), 2 (CL-2), 3 (CL-3), 4 (RL)
39	J_1	Discrete	0 (PJ), 1 (CJ), 2 (RJ)
...
69	J_{31}	Discrete	0 (PJ), 1 (CJ), 2 (RJ)

Table 3 Beam elements for different states of link modules

Link module	Beam element	
	In-plane width (mm)	Young's modulus
Absent	1×10^9	1×10^{-13} Pa
CL-1	0.5	1.4 GPa
CL-2	1.0	1.4 GPa
CL-3	1.5	1.4 GPa
RL	7.5	1.4 GPa

configuration as interpreted consists of five RLs (besides the ground link), four PJs, and two RJs. The motion of the mechanism is due to the relative rotation permitted by the PJs. Furthermore, the mechanism in Fig. 11(b) is equivalent to a rigid-body four-bar mechanism (Fig. 11(c)) because the clamped RL3 can be removed and the rigidly connected RL2 and RL1 can be viewed as one RL. The kinematic degree-of-freedom of the mechanism was correctly limited to one due to the appropriate use of RJs and PJs, although five RLs (besides the ground link) were used. Thus, it can be concluded that, on the one hand, PJs provide an RBM with mobility; on the other hand, RJs and PJs together provide an RBM with the correct number of degrees-of-freedom.

The first row and second row of Fig. 12 depict the interpretations of the results of examples II and III, respectively. The first column, second column, and third column show the link and joint modules of the original resulting mechanisms, of the mechanisms (as interpreted according to the joint interpretation principles), and of the deformed configurations of the mechanisms (as interpreted), respectively.

The fully compliant path generator of example II (Fig. 12(b)), as interpreted, consists of five CLs, three CJs, and three RJs. No PJ appeared in the result. As seen from the deformed configuration (Fig. 12(c)), the CJs permit the relative rotation (deformation of CJs) between the connected links and transmit bending moments. Both the rotational deformation of the CJs and the bending deformation of the CLs contribute to the motion of the mechanism.

The partially compliant path generator of example III (Fig. 12(e)), as interpreted, consists of eight CLs, two RLs, six PJs, six CJs, and three RJs. All the five basic modules appear in the result. As seen from the deformed configuration (Fig. 12(f)), the RLs and RJs do not have any deformation, the PJs permit relative rotations between the links without transmitting the moments, and the CJs permit relative rotations with the moment transmission. All the modules function as they were defined.

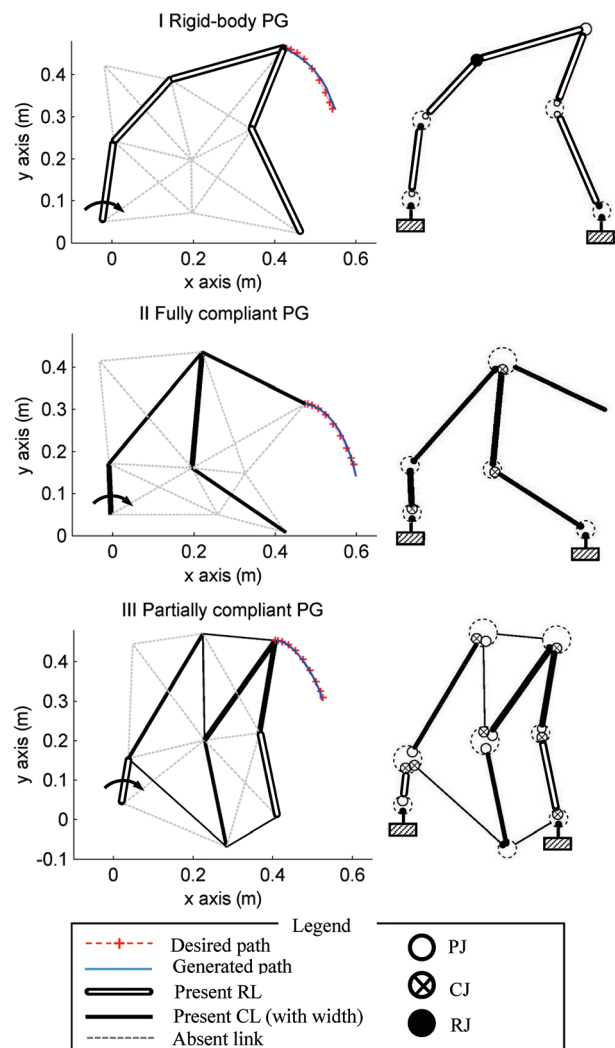


Fig. 10 Design results of examples I-III

The model used in the module optimization process is essentially an implicit model which keeps the removed links and joints with elements of very small stiffness so that their effects on the properties of the mechanism are negligible. This implicit model may result in errors in analysis and thus needs to be verified.

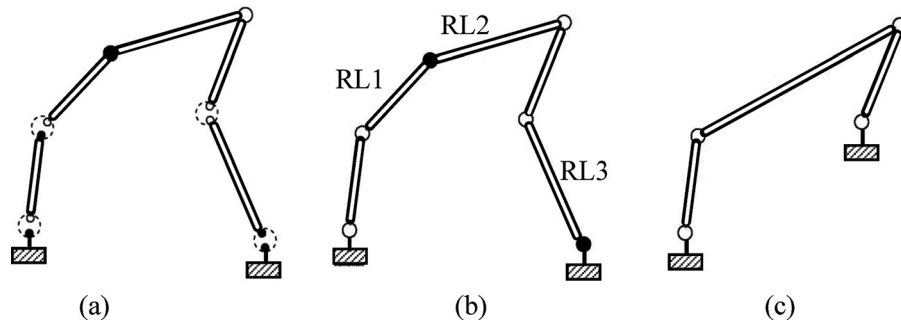


Fig. 11 Result interpretation of example I—rigid-body path generator: (a) the joint and link modules of the original result mechanism, (b) the interpreted joint and link modules of the mechanism, and (c) the equivalent four-bar RBM

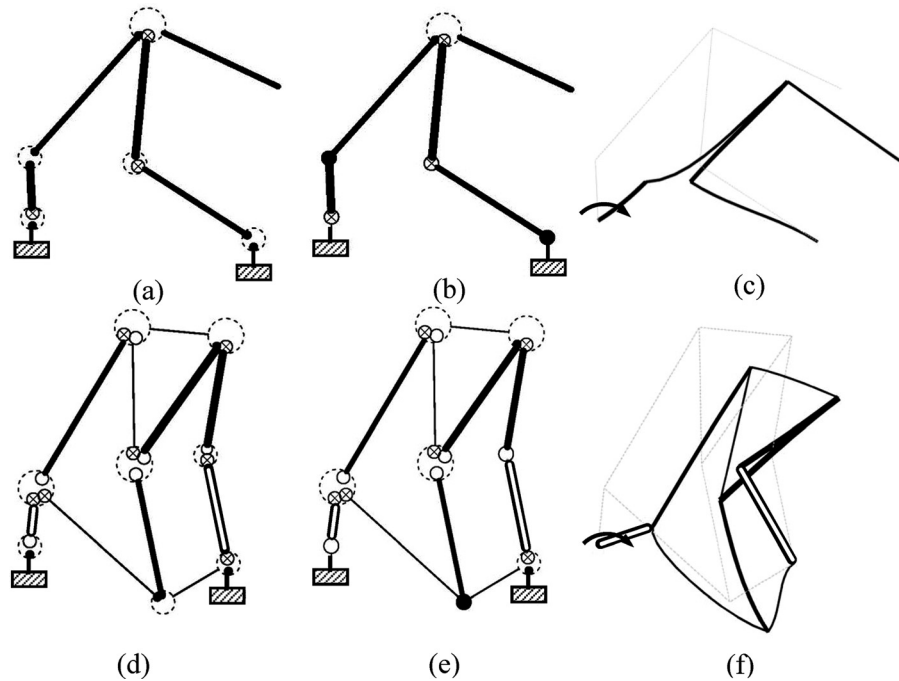


Fig. 12 Results of examples II (the first row) and III (the second row): (a) and (d) represent the original design results; (b) and (e) represent the results with interpretation; and (c) and (f) represent the deformed configurations of the mechanisms

Taking the design result of example III for example, the generated path based on the implicit model and the generated path based on the explicit model (the removed links are not kept in the stiffness matrix) are almost the same (as shown in Fig. 13), which means that the implicit model is accurate enough for the proposed module optimization approach. Note that in the explicit model, each link of the mechanism was discretized into three beam elements to ensure accuracy.

7 Conclusions

A module view of mechanisms was proposed to generally represent RBMs, fully CMs, and partially CMs with five basic modules: CLs, RLs, PJs, CJs, and RJs. Then, a finite-element model of both RBMs and CMs was established with the beam-hinge strategy to mesh the design domain, which consists of the beam element and the hinge element in a finite-element approach (SPACAR). Subsequently, the concept of topology optimization was taken to form a module optimization process, particularly to determine the states (removed or remaining) of modules in the design domain. The salient merits of introducing the hinge element include: (1) a natural way to describe various types of connections between two

elements or modules and (2) a provision of the possibility to specify rotational input motion in a design problem.

The module optimization approach covers both the so-called link determination approach and the joint determination approach to the concurrent type and dimensional synthesis of mechanisms in the literature. With the module optimization approach, one may obtain an RBM, a partially CM, or a fully CM for a given mechanical task. The states of the joints and links do not need to be predetermined, which are more general than both the joint determination approach and the link determination approach in the literature. Furthermore, this approach also enables designers to prescribe the types of modules prior to the design phase to obtain desired categories of mechanisms. Additionally, this study demonstrates the first time that CJs are considered as the basic components in the type and dimensional synthesis of CMs, though many CJs for large rotation have been designed and used in practice.

The proposed approach sets a foundation for the type and dimensional synthesis of RBMs and CMs. With this foundation, it is possible to design mechanisms for other functional requirements, such as function generation, motion generation, or shape morphing.

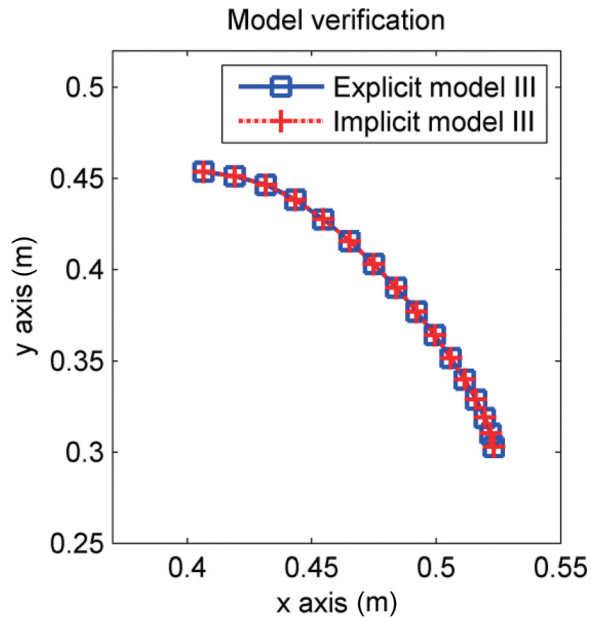


Fig. 13 Models based on the explicit model and the implicit model for the result of example III

In this study, a CJ was modeled with a hinge element that only describes the rotational stiffness of a CJ. The limitations of this model are listed below:

- (1) The stiffness in translational directions was assumed to be infinite, i.e., a CJ is rigid in translational directions (two beams connected by a CJ can only have relative rotation but not relative translation). This approximation is reasonable when a CJ is designed with lower rotational stiffness and higher translational stiffness. Some of these CJs can be found in Refs. [26,27,30,37].
- (2) Although conventional notch-type CJs can only travel over small limited ranges, the angular travel of a CJ in this study was assumed to cover a large angle (60 deg) without yield failure. Refer to Refs. [26,27,30,37] for CJs with large travel angles.
- (3) The size and physical construction of a CJ were not considered.
- (4) Multiple joints may appear at the same connection point (location). This limitation may require special treatments to locate these joints; otherwise, the model is an approximation.

Acknowledgment

The authors acknowledge the partial financial support from the NSERC Discovery Grant and the Chinese CSC. We also thank Professor Jaap Meijaard from the University of Twente (The Netherlands) for providing the advanced version of SPACAR and for his instructions on the use of SPACAR.

References

- [1] Howell, L. L., 2001, *Compliant Mechanisms*, Wiley, New York.
- [2] Erdman, A. G., and Sandor, G. N., 1997, *Mechanism Design: Analysis and Synthesis*, Prentice-Hall, Englewood Cliffs, NJ.
- [3] Freudenstein, F., and Dobrjanskyj, L., 1966, "On a Theory for the Type Synthesis of Mechanisms," *Applied Mechanics*, H. Görtler, ed., Springer, Berlin, pp. 420–428.
- [4] Zhang, W. J., and Li, Q., 1999, "On a New Approach to Mechanism Topology Identification," *ASME J. Mech. Des.*, **121**(1), pp. 57–64.
- [5] Kawamoto, A., Bendsøe, M. P., and Sigmund, O., 2004, "Articulated Mechanism Design With a Degree of Freedom Constraint," *Int. J. Numer. Methods Eng.*, **61**(9), pp. 1520–1545.

- [6] Kawamoto, A., 2005, "Path-Generation of Articulated Mechanisms by Shape and Topology Variations in Non-Linear Truss Representation," *Int. J. Numer. Methods Eng.*, **64**(12), pp. 1557–1574.
- [7] Eberhard, P., Gaugele, T., and Sedlaczek, K., 2009, "Topology Optimized Synthesis of Planar Kinematic Rigid Body Mechanisms," *Advanced Design of Mechanical Systems: From Analysis to Optimization*, J. A. C. Ambrosio and P. Eberhard, eds., Springer-Verlag, Vienna, Austria, pp. 287–302.
- [8] Eberhard, P., and Sedlaczek, K., 2009, "Grid-Based Topology Optimization of Rigid Body Mechanisms," *Advanced Design of Mechanical Systems: From Analysis to Optimization*, J. C. Ambrósio and P. Eberhard, eds., Springer, Vienna, Austria, pp. 303–315.
- [9] Sedlaczek, K., and Eberhard, P., 2009, "Topology Optimization of Large Motion Rigid Body Mechanisms With Nonlinear Kinematics," *ASME J. Comput. Nonlinear Dyn.*, **4**(2), p. 021011.
- [10] Kim, Y. Y., Jang, G.-W., Park, J. H., Hyun, J. S., and Nam, S. J., 2006, "Automatic Synthesis of a Planar Linkage Mechanism With Revolute Joints by Using Spring-Connected Rigid Block Models," *ASME J. Mech. Des.*, **129**(9), pp. 930–940.
- [11] Ananthasuresh, G. K., 1994, "A New Design Paradigm for Micro-Electro-Mechanical Systems and Investigations on the Compliant Mechanisms," Ph.D. thesis, University of Michigan, Ann Arbor, MI.
- [12] Joo, J., Kota, S., and Kikuchi, N., 2000, "Topological Synthesis of Compliant Mechanisms Using Linear Beam Elements," *Mech. Struct. Mach.*, **28**(4), pp. 245–280.
- [13] Joo, J. Y., and Kota, S., 2004, "Topological Synthesis of Compliant Mechanisms Using Nonlinear Beam Elements," *Mech. Based Des. Struct. Mach.*, **32**(1), pp. 17–38.
- [14] Frecker, M. I., Ananthasuresh, G. K., Nishiwaki, S., Kikuchi, N., and Kota, S., 1997, "Topological Synthesis of Compliant Mechanisms Using Multi-Criteria Optimization," *ASME J. Mech. Des.*, **119**(2), p. 238.
- [15] Ramrakhiani, D., Frecker, M., and Lesieur, G., 2009, "Hinged Beam Elements for the Topology Design of Compliant Mechanisms Using the Ground Structure Approach," *Struct. Multidiscip. Optim.*, **37**(6), pp. 557–567.
- [16] Yu, J., Li, S., Su, H., and Culpepper, M. L., 2011, "Screw Theory Based Methodology for the Deterministic Type Synthesis of Flexure Mechanisms," *ASME J. Mech. Rob.*, **3**(3), p. 031008.
- [17] Hopkins, J. B., and Culpepper, M. L., 2010, "Synthesis of Multi-Degree of Freedom, Parallel Flexure System Concepts Via Freedom and Constraint Topology (FACT)—Part I: Principles," *Precis. Eng.*, **34**(2), pp. 259–270.
- [18] Su, H. J., Dorozhkin, D. V., and Vance, J. M., 2009, "A Screw Theory Approach for the Conceptual Design of Flexible Joints for Compliant Mechanisms," *ASME J. Mech. Rob.*, **1**(4), pp. 1–8.
- [19] Kim, C. J., Kota, S., and Moon, Y. M., 2006, "An Instant Center Approach Toward the Conceptual Design of Compliant Mechanisms," *ASME J. Mech. Des.*, **128**(3), pp. 542–550.
- [20] Cao, L., Dolovich, A. T., and Zhang, W. J., 2015, "Hybrid Compliant Mechanism Design Using a Mixed Mesh of Flexure Hinge Elements and Beam Elements Through Topology Optimization," *ASME J. Mech. Des.*, **137**(9), p. 092303.
- [21] He, P. R., Zhang, W. J., Li, Q., and Wu, F. X., 2003, "A New Method for Detection of Graph Isomorphism Based on the Quadratic Form," *ASME J. Mech. Des.*, **125**(3), pp. 640–642.
- [22] Kong, F. G., Li, Q., and Zhang, W. J., 1999, "An Artificial Neural Network Approach to Mechanism Kinematic Chain Isomorphism Identification," *Mech. Mach. Theory*, **34**(2), pp. 271–283.
- [23] Murphy, M. D., Midha, A., and Howell, L. L., 1996, "The Topological Synthesis of Compliant Mechanisms," *Mech. Mach. Theory*, **31**(2), pp. 185–199.
- [24] van der Werf, K., 1977, "Kinematic and Dynamic Analysis of Mechanisms: A Finite Element Approach," Ph.D. dissertation, Delft University of Technology, Delft, The Netherlands.
- [25] Deepak, S. R., Dinesh, M., Sahu, D. K., and Ananthasuresh, G. K., 2009, "A Comparative Study of the Formulations and Benchmark Problems for the Topology Optimization of Compliant Mechanisms," *ASME J. Mech. Rob.*, **1**(1), p. 011003.
- [26] Trease, B. P., Moon, Y. M., and Kota, S., 2004, "Design of Large-Displacement Compliant Joints," *ASME J. Mech. Des.*, **127**(4), pp. 788–798.
- [27] Martin, J., and Robert, M., 2011, "Novel Flexible Pivot With Large Angular Range and Small Center Shift to Be Integrated Into a Bio-Inspired Robotic Hand," *J. Intell. Mater. Syst. Struct.*, **22**(13), pp. 1431–1437.
- [28] Dao, T. P., and Huang, S. C., 2013, "Design and Analysis of Compliant Rotary Joint," *Appl. Mech. Mater.*, **372**, pp. 467–470.
- [29] Hou, C. W., and Lan, C. C., 2013, "Functional Joint Mechanisms With Constant-Torque Outputs," *Mech. Mach. Theory*, **62**, pp. 166–181.
- [30] Kang, D., and Gweon, D., 2013, "Analysis and Design of a Cartwheel-Type Flexure Hinge," *Precis. Eng.*, **37**(1), pp. 33–43.
- [31] Jonker, J. B., 1989, "A Finite Element Dynamic Analysis of Spatial Mechanisms With Flexible Links," *Comput. Methods Appl. Mech.*, **76**(1), pp. 17–40.
- [32] Zhang, W. J., and van der Werf, K., 1998, "Automatic Communication From a Neutral Object Model of Mechanism to Mechanism Analysis Programs Based on a Finite Element Approach in a Software Environment for CAD/CAM of Mechanisms," *Finite Elem. Anal. Des.*, **28**(3), pp. 209–239.
- [33] Zhang, W. J., 1994, "An Integrated Environment for CAD/CAM of Mechanical Systems," Ph.D. dissertation, Delft University of Technology, Delft, The Netherlands.
- [34] Hetrick, J. A., 1999, "An Energy Efficiency Approach for Unified Topological and Dimensional Synthesis of Compliant Mechanisms," Ph.D. dissertation, University of Michigan, Ann Arbor, MI.

- [35] Norton, R. L., 2004, *Design of Machinery: An Introduction to the Synthesis and Analysis of Mechanisms and Machines*, McGraw-Hill Higher Education, New York.
- [36] Aarts, R. G. K. M., Meijaard, J. P., and Jonker, J. B., 2011, "SPACAR User Manual," University of Twente, Enschede, The Netherlands, Report No. WA-1299.
- [37] Riverhawk Company, 2014, "Flexural Pivots," <http://direct.daitron.co.jp/pdf/Riverhawk-FlexuralPivotCatalog.pdf>
- [38] MathWorks, 2015, "Global Optimization Toolbox User's Guide (R2015a)," http://www.mathworks.com/help/pdf_doc/gads/gads_tb.pdf
- [39] Goldberg, D. E., 1989, *Genetic Algorithms in Search, Optimization, and Machine Learning*, Longman Publishing, Boston, MA.